International Journal of Molecular Sciences

MDPI

Article

Transforming Growth Factor-β3 Chitosan Sponge (TGF-β3/CS) Facilitates Osteogenic Differentiation of Human Periodontal Ligament Stem Cells

Yangfan Li [1], Zhifen Qiao [1], Fenglin Yu [1], Huiting Hu [2], Yadong Huang [1], Qi Xiang [1,*], Qihao Zhang [1], Yan Yang [1] and Yueping Zhao [2]

[1] Institute of Biomedicine and Guangdong Provincial Key Laboratory of Bioengineering Medicine, Jinan University, Guangzhou 510632, PR China

[2] Department of Stomatology, Jinan University Medical College, Guangzhou 510632, China

Yangfan Li and Zhifen Qiao contributed equally to this work.

* Correspondence: Qi Xiang, Institute of Biomedicine and Guangdong Provincial Key Laboratory of Bioengineering Medicine, Jinan University, Guangzhou 510632, PR China, E-mail address: txiangqi@jnu.edu.cn (Q Xiang).

Received: date; Accepted: date; Published: date

Abstract: Periodontal disease is the main reason for tooth loss in adults. Tissue engineering and regenerative medicine are the advanced technologies used to manage soft and hard tissue defects caused by periodontal disease. We developed a transforming growth factor-β3 chitosan sponge (TGF-β3/CS) to repair periodontal soft and hard tissue defects. We investigated the proliferation and osteogenic differentiation behaviors of primary human periodontal ligament stem cells (hPDLSCs) to discuss the bioactivity and application of TGF-β3 in periodontal disease. We separately used Calcein-AM/PI double-labeling or CM-Dil-labeling coupled with fluorescence microscopy to trace the survival and function of the cells after implantation in vitro or in vivo. The mineralization of osteogenic differentiated hPDLSCs was confirmed by measuring ALP activity and calcium content. The levels of COL I, ALPL, TGF-βRI, TGF-βRII, and Pp38/t-p38 were tested using Western blot to explore the mechanism of bone repair prompted by TGF-β3. When hPDLSCs were inoculated with different concentrations of TGF-β3/CS (62.5–500 ng/mL), ALP activity was the highest in TGF-β3 (250 ng/mL) group after seven days ($P < 0.05$ vs. control); the calcium content in each group increased significantly after 21 and 28 days ($P < 0.001$ vs. control). The best result was achieved in the TGF-β3 (500 ng/mL) group. All results showed that TGF-β3/CS can promote osteogenic differentiation of hPDLSC and may be involved in the p38 MAPK signaling pathway. TGF-β3/CS has the potential for application in the repair of incomplete alveolar bone defects.

Keywords: transforming growth factor β3; chitosan sponge; human periodontal ligament cells; osteogenic differentiation

Graphical Abstract

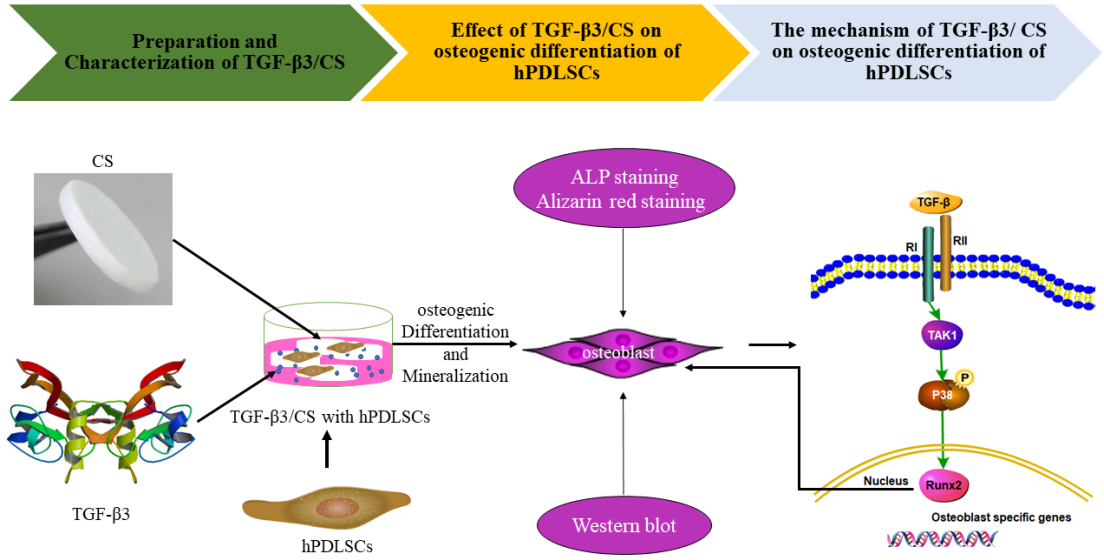

1. Introduction

Periodontal disease is a chronic inflammatory condition that affects the supporting tissues around the teeth, resulting in periodontal tissue breakdown or tooth loss in severe cases. Being highly prevalent among adults, periodontal disease treatment is receiving increased attention from researchers and clinicians [1]. Therefore, repairing periodontal support tissues such as alveolar bone is an indispensable part of the treatment of periodontal disease. With the increasing popularity of dental implant surgery, the lack of bone mass in patients with periodontitis has limited the need for implant surgery, and the need for repair of alveolar bone defects is increasing [2,3].

The current clinical techniques mainly used for the treatment of alveolar bone defects [4] are bone grafting and guided bone regeneration (GBR). Autologous bone grafting is considered to be the gold standard of bone repair [5-8], but it has many limitations, such as longer operation and recovery times, patients with insufficient bone mass, and a number of complications are possible [9,10]. GBR uses a barrier to provide space and is filled with new bone to compensate for these deficiencies [11,12]. However, GBR has shortcomings such as immune rejection, and poor morphological structure and mechanical properties [13-15]. In recent years, periodontal tissue engineering technology, characterized by the use of (stem) cells, bioactive molecules (e.g., growth factors), and scaffold materials as the three basic elements, has provided a new solution for reconstructing alveolar bone defects.

Transforming growth factor-β3 (TGF-β3) has been used for cartilage repair, tissue regeneration and wound healing in vivo [16-18]. TGF-β3 facilitates matrix formation, immunity, as well as maintenance of stem cell characteristics [19]. TGF-β promotes the proliferation and early differentiation of mesenchymal stem cells (MSCs) into osteoblasts, chondrocytes, adipocytes and tendon cells [20]. TGF-β3 can also recruit endogenous mesenchymal stem cells to initiate bone regeneration [21-24]. TGF-β3 can induce endochondral bone formation [25] and complete bone remodeling [26]. It may play a profound role in some osteogenic stages, so TGF-β3 can be considered a selective bioactive molecule for repairing alveolar bone defects. Moioli et al. [27] demonstrated for the first time that autologous MSCs and controlled-release TGF-β3 can reduce the surgical trauma due to local osteotomy. However, TGF-β3 is easily degrades, inactivates, and spreads. Therefore, it was necessary to develop some carrier materials to carry it. Chitosan is a natural polymer material that can effectively promote wound healing and early osteogenesis after tooth extraction [28]. It would be an ideal carrier of TGF-β3.

Alveolar bone regeneration is enhanced by the addition of osteogenic cells to biomaterial scaffolds, which can reduce treatment time and produce better outcomes and increase patient comfort [29]. Periodontal ligament stem cells (PDLSCs) promote osteoblastic and osteoclastic differentiation

of osteoblast, and form an ectopic cementum/ligament-like complex [30]. Kim et al. [31] reported that the growth and induction of PDLSCs promote the regeneration of cementum and periodontal ligament, to enable easy root fixation and resorption. As PDLSC is one the suitable stem cells for periodontal tissue regeneration, we employed hPDLSCs to validate TGF-β3 in regeneration of alveolar bone defects.

By comparison of our results with those reported previously, we found that PDLSCs undergo osteogenic differentiation through the mitogen-activated protein kinase (MAPK) signaling pathway [32-34], and that signaling transduction mediated by TGF-β3 in osteogenic differentiation and bone regeneration [35] specifically occurs through both canonical Smad-dependent pathways (TGF-β ligands, receptors, and Smads) and non-canonical Smad-independent signaling pathway (e.g., p38 MAPK pathway). We hypothesized that TGF-β3 may promote osteogenic differentiation of hPDLSCs via the p38 MAPK pathway. So, we tested the levels of COL I, ALPL, TGF-βRI, TGF-βRII, and Pp38/p38 by Western blot.

TGF-β3/CS facilitated the osteogenic differentiation of hPDLSCs in this study. We further examined and verified the mechanism through which TGF-β3 promotes osteogenic differentiation of hPDLSCs. TGF-β3 may be combined with hPDLSCs for the regeneration of alveolar bone defects.

2. Results

2.1. Preparation and Characterization of TGF-β3/CS

As shown in Figure 1A, CS has a regular appearance and a smooth surface. In the SEM image, TGF-β3/CS showed a three-dimensional (3D) porous network structure, and interpenetrating pore structures resulted in a large internal surface area (Figure 1B). The pore size of the TGF-β3/CS was 156.95 ± 18.21μm, the water absorption was 2347% ± 201%, the swelling ratio was 52.67% ± 12.42%, and the porosity was 85.65% ± 3.5%.

As shown in Figure 1C, TGF-β3 can be stably released from CS at predetermined time points, cumulatively released in CS, and continues to act on the cells (Figure 1D). The biocompatibility of the TGF-β3/CS was evaluated using the MTT assay. Compared with the control group, the scaffold had no obvious cytotoxicity ($P > 0.05$; Figure 1E). Therefore, CS is a suitable carrier of TGF-β3, ensuring sustained and stable release of TGF-β3 in vivo and in vitro.

After hPDLSCs were cultured on TGF-β3/CS for three days, hPDLSCs grew well. The cell structure was intact, and there were more viable cells (Figure 2A, green) than dead cells (Figure 2A, red). TGF-β3/CS with hPDLSCs pre-stained with CM-Dil were implanted subcutaneously into SD rats for 7, 14, and 21 days to observe the growth of cells (Figure 2B). The red viable cells were also observed after 21 days, indicating that TGF-β3/CS with hPDLSCs can survive well in animals.

After hPDLSCs were seeded in TGF-β3/CS for seven days, hPDLSCs displayed good adhesion and extension state on the surface of CS, and the cells adhered to each other to form a sheet growth, and some cells crossed the pores of the porous sponge (Figure 2C). After inoculation of hPDLSCs on CS with different concentrations of TGF-β3, we observed that hPDLSCs could grow and proliferate on CS ($P < 0.001$ vs. control; Figure 2D).

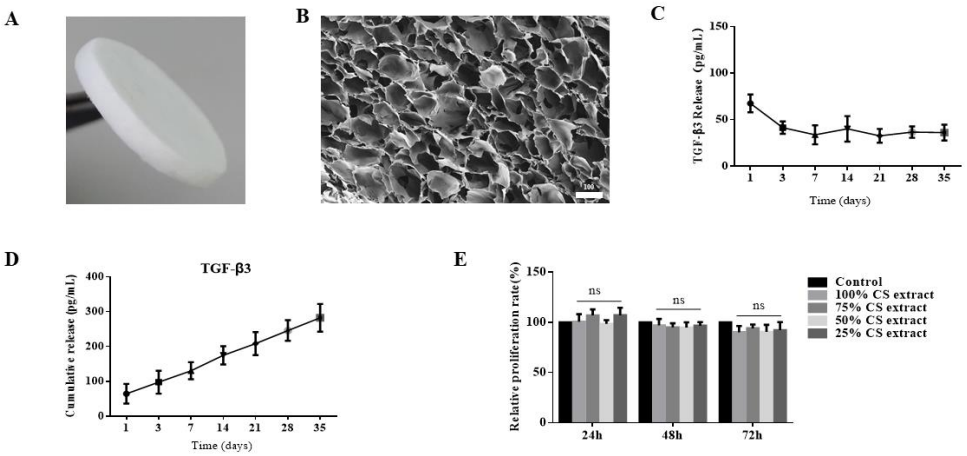

Figure 1. Characterization of TGF-β3/CS and Release of TGF-β3 from CS. (A). CS photographs. (B). The scanning electron microscope (SEM) CS image. Scale bar represents 100 μm. (C). The release curve of TGF-β3 from CS (mean ± SD; *n* = 3). (D). The cumulative release of TGF-β3 from CS (mean ± SD; *n* = 3). (E). Cytotoxicity assay of CS extract measured by MTT assay (mean ± SD; n = 5). Blank control group: cells were cultured only with the extraction medium; CS extract group: cells were cultured with 25%, 50%, 75%, or 100% CS extract.

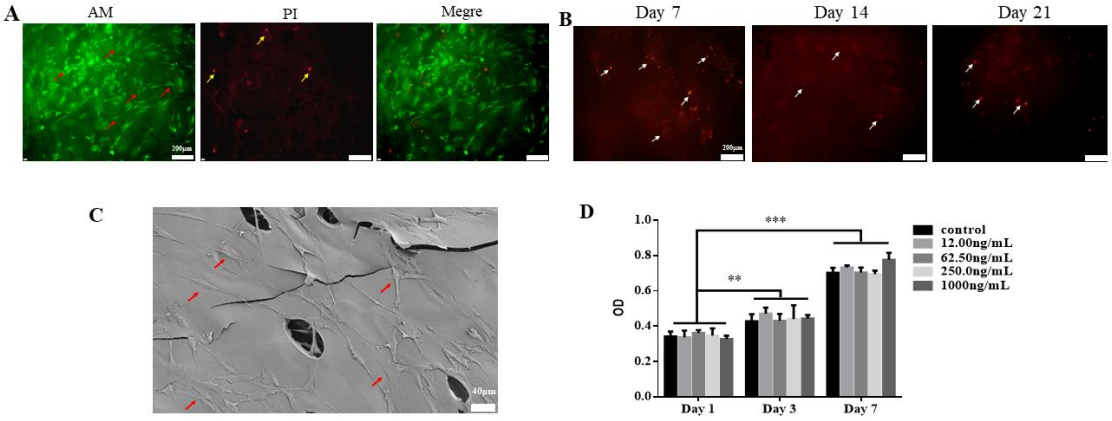

Figure 2. Effect of TGF-β3/CS on the growth and proliferation of hPDLSCs. (A) Calcein-AM staining of hPDLSCs on TGF-β3/CS after three days of culture; live cells (red arrow) are stained by AM (green), and dead cells (yellow arrow) are stained by PI (red). Scale bar represents 200 μm. (B) TGF-β3/CS with hPDLSCs (white arrow) implant Sprague-Dawley rats for 7, 14, and 21 days, and then stained with CM-Dil (red). The cell survival was observed using a fluorescence microscope. (C) SEM photomicrographs of hPDLSCs (red arrow) in CS for seven days. Scale bar represents 40 μm. (D) hPDLSCs growth in TGF-β3/CS was measured by CCK-8 (mean ± SD; n = 5). *P < 0.05 vs. control; * * P < 0.01 vs. control; *** P < 0.001 vs. control.

2.2. TGF-β3 Does Not Affect Growth and Proliferation of hPDLSCs but Facilitates Its Osteogenic Differentiation

The relative proliferation rate of hPDLSCs cultured at different concentrations of TGF-β3 for 24, 48, and 72 h was examined using the MTT assay. The relative proliferation rates depended on time, but they did not change with the concentration of TGF-β3. TGF-β3 did not significantly promote or inhibit the growth or proliferation of hPDLSCs within the concentration gradient range ($P > 0.05$, vs. control), and the high concentration showed no significant toxicity to hPDLSCs (Figure 3A). However, as shown in Figure 3B, TGF-β3 promoted ALP secretion and calcium deposition of hPDLSCs. When the loading of TGF-β3 was 250 or 500 ng/mL, the expressions of ALP and calcium in hPDLSCs were

significantly up-regulated. The optimal concentration range of TGF-β3 in promoting cell differentiation is 250–500 ng/mL.

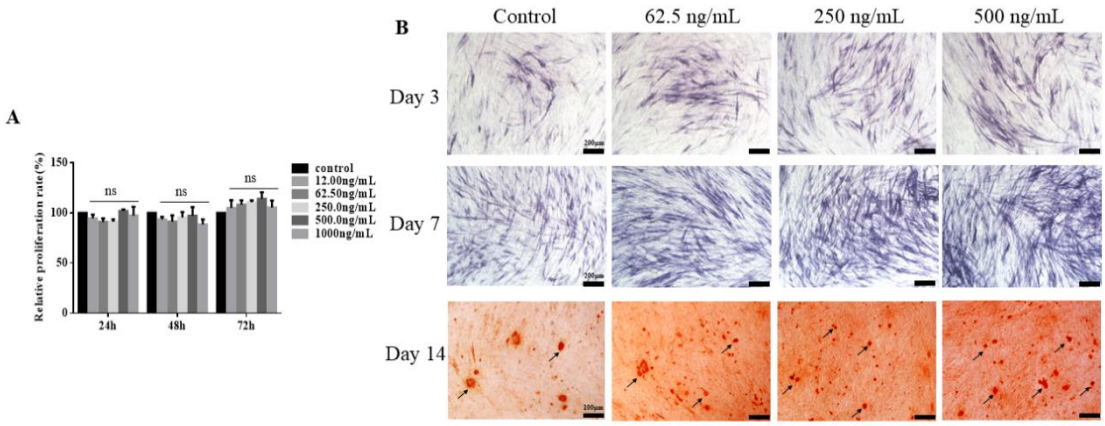

Figure 3. TGF-β3 does not affect the growth and proliferation of hPDLSCs, but can promote its osteogenic differentiation. (A). The relative proliferation rate of hPDLSCs cultured at different concentrations of TGF-β3 for 24 h, 48 h and 72 h by MTT assay (n=5). (B). Alkaline phosphatase (ALP) staining (purple) was used to detect the ALP activity of hPDLSCs with different concentrations of TGF-β3 after 3 days and 7 days of osteogenic induction; Alizarin red staining (red) was used to detect the calcium content of hPDLSCs with different concentrations of TGF-β3 after 14 days of osteogenic induction. Black arrow shows calcium deposition.

2.3. TGF-β3/CS Facilitates Osteogenic Differentiation of hPDLSCs

hPDLSCs were inoculated on CS with different concentrations of TGF-β3 (62.5, 250, and 500 ng/mL), and ALP values were determined for 3, 7, and 14 days after osteoblastic induction (Figure 4A). We observed no significant difference in any TGF-β3/CS group compared with CS for three days, but TGF-β3/CS groups exhibited significant differences after 7 and 14 days ($P < 0.05$, vs. control; Figure 4B).

The calcium content was measured after osteogenic induction for 14, 21, and 28 days. No significant differences we observed in any groups for 14 days, but every TGF-β3/CS group had significantly higher levels of calcium content for 21 and 28 days ($P < 0.05$, vs. control). The best results were recorded for the TGF-β3 (500 ng/mL)/CS group ($P < 0.001$, vs. control) (Figure 4C).

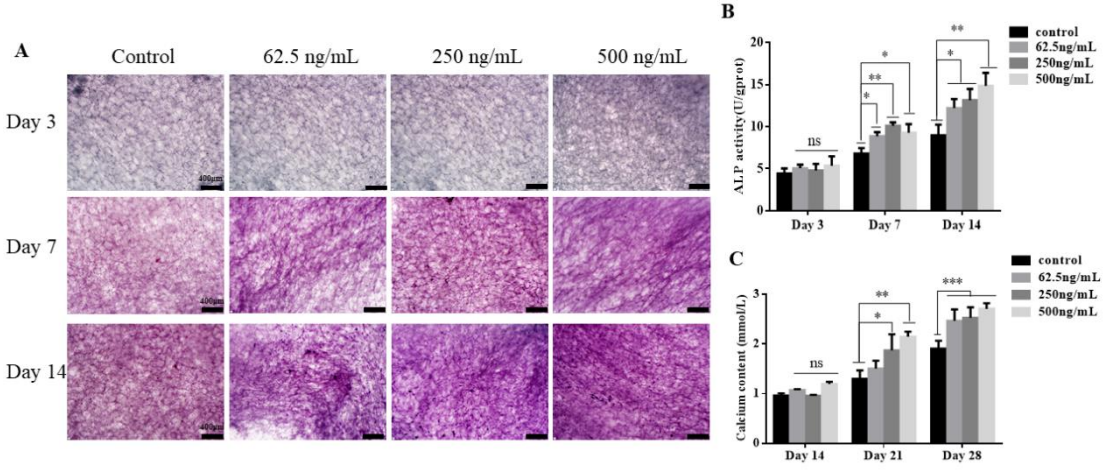

Figure 4. Effect of TGF-β3/CS on osteogenic differentiation of hPDLSCs. (A). ALP staining (purple) was used to detect the ALP activity of hPDLSCs on CS with different concentrations of TGF-β3 after 3 days, 7 days and 14 days of osteogenic induction. (B). Detection of ALP activity of hPDLSCs on CS with different concentrations of TGF-β3 after 3 days, 7 days and 14 days of osteogenic induction. (C).

Determination of calcium of hPDLSCs on CS with different concentrations of TGF-β3 after 14d, 21d and 28d of osteogenic induction(n=3). * P < 0.05 vs. control; * * P < 0.01 vs. control.; *** P < 0.001 vs. control.

2.4. TGF-β3 Promotes Osteogenic Differentiation of hPDLSCs via p38 MAPK Pathway

To verify the effect of TGF-β3 on osteogenic differentiation of hPDLSCs, we examined the changes in osteogenic-associated proteins (COL I, COL II, and ALPL) and pathway proteins (TGF-βRI, TGF-βRII, p38, Pp38, and Runx2) with induction time and TGF-β3 concentration via Western blot (Figures 5A and 6B). There was a statistically significant difference in the increase in COLI expression in the TGF-β3 (500 ng/mL) induction group after 7 and 14 days' induction ($P < 0.001$, vs. control), whereas the other induction groups showed no statistical differences ($P > 0.05$, vs. control). The amount of COLI expression induced after 14 days was significantly higher than that after 7 days (Figure 5B).

The expression of COL II significantly increased in TGF-β3 (125, 250, and 500 ng/mL) induction groups after seven days' induction ($P < 0.001$, vs. control); after 14 days, there was no statistical difference in the induction groups ($P > 0.05$, vs. control). Compared with the day 7 results, TGF-β3 (125, 250, and 500 ng/mL) induction groups for day 14 were significantly reduced (Figure 5C).

The expression of ALPL was significantly decreased in the TGF-β3 (500 ng/mL) induction groups after 7 and 14 days of induction ($P < 0.01$, vs. control), and no significant difference was found in the other groups ($P > 0.05$, vs. control). The ALPL expression induced for 14 days was significantly lower than that for 7 days (Figure 5D).

In conclusion, as the induction time increased, the COL I of the TGF-β3 (500 ng/mL) induction group increased significantly, and the COL II and ALPL decreased significantly.

The expression of TGF-βRI was significantly increased in TGF-β3 (500 ng/mL) induction groups after 7 and 14 days' induction ($P < 0.001$, vs. control). The expression of TGF-βRI induced for 14 days was significantly higher than for 7 days (Figure 6C). The expression of TGF-βRII in the TGF-β3 (500 ng/mL) induction group was significantly increased after 7 and 14 days' induction. ($P < 0.001$, vs. control). The TGF-βRII expression induced for 14 days was significantly lower than for 7 days (Figure 6D). No significant difference was found in the expression of t-p38 in the induction group after 7 and 14 days' induction ($P > 0.05$, vs. control) (Figure 6E), whereas the expression of Pp38 was significantly increased in the TGF-β3 (500 ng/mL) induction group ($P < 0.001$, vs. control). The Pp38 induced for 14 days was significantly higher than for 7 days (Figure 6F). The expression of Runx2 in the TGF-β3 (500 ng/mL) induction group was significantly increased after seven days of induction ($P < 0.001$, vs. control); after 14 days, no statistical difference was found in the induction group ($P > 0.05$, vs. control). The expression of Runx2 induced for 14 days was significantly lower than for 7 days (Figure 6G).

In conclusion, as the induction time increased, TGF-βRI and Pp38 in the TGF-β3 (500 ng/mL) induction group increased significantly, the TGF-βRII and Runx2 decreased significantly, and t-p38 was unchanged (Figure 6C). So, Pp38/t-p38 showed an up-regulated trend, indicating that TGF-β3 can significantly increase osteogenic differentiation of hPDLSCs.

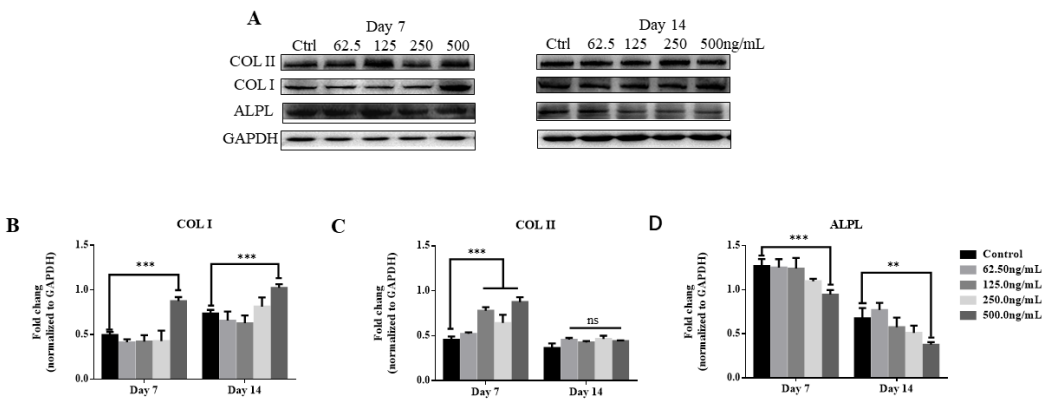

Figure 5. Expression and analysis of proteins associated with osteogenic differentiation. (A-D) After osteogenic induction of hPDLSCs with different concentrations of TGF-β3 for 7 and 14 days, the expression of osteogenic proteins (COL I, COL II, and ALPL) were detected by (A) Western blot and analyzed by gray scale scanning for (B) COL I, (C) COL II and (D) ALPL (n = 3). * P < 0.05 vs. control; * * P < 0.01 vs. control.; *** P < 0.001 vs. control. Abbreviations: Col I , type I collagen; Col II, type II collagen; ALPL, Alkaline phosphatase.

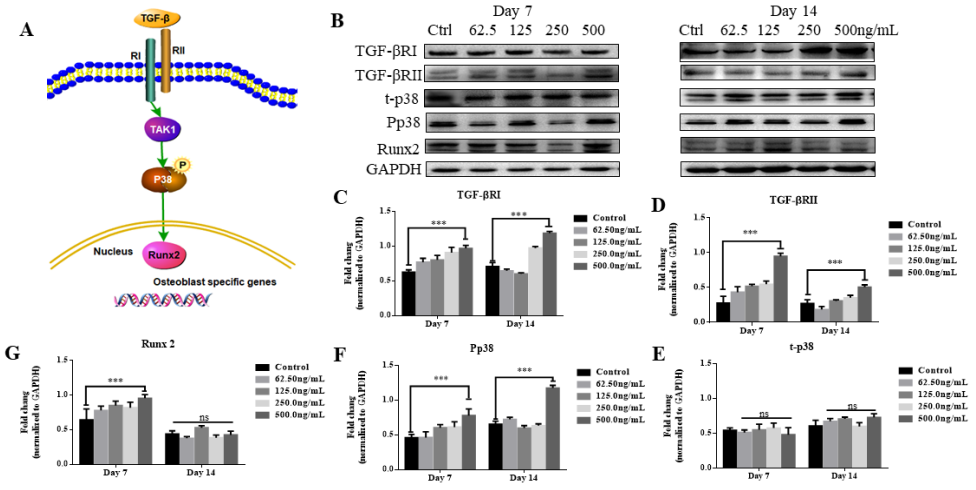

Figure 6. The mechanism of TGF-β3 on osteogenic differentiation of hPDLSCs based on this study. (A) Schematic representation of the mechanism of TGF-β3 on osteogenic differentiation of hPDLSCs. (B) After osteogenic induction of hPDLSCs with different concentrations of TGF-β3 for 7 and 14 days, the expression of osteogenic pathway proteins were detected by (B) Western blot and analyzed by gray scale scanning for (C) TGF-βRI, (D) TGF-βRII, (E) t-p38, (F) Pp38 and (G) Runx2 (n=3).* P < 0.05 vs. control; * * P < 0.01 vs. control; *** P < 0.001 vs. control. Abbreviations: TGF-βRI, transforming growth factor-β receptor I; TGF-βRII, transforming growth factor-β receptor II; t-p38, total p38; Pp38, phosphorylated p38; Runx2, runtrelated transcription factor 2.

3. Discussion

The aim of periodontal tissue engineering is to regenerate the tooth's supporting tissue through a combination of proper biomaterials, such as growth factors and scaffold materials, which stimulate cells and signaling molecules to produce new healthy tissue.

PDLSCs have broad application prospects as odontogenic seed cells in periodontal tissue engineering and regenerative medicine due to their biosafety and odontogenic properties. Biomaterials that repair alveolar bone defects require stable biological properties and good biocompatibility. Many studies had examined the use of TGF-β3 for cartilage repair, tissue regeneration, and wound healing in vivo [36]. In this study, we prepared TGF-β3/CS freeze-dried sponge, which is a high-porosity network material with good water absorption and swelling rate. It can mimic the natural extracellular microenvironment of dental tissue and promote the adhesion, proliferation, and differentiation of hPDLSCs. The morphology and Calcein-AM/PI double staining results showed that hPDLSCs can be spread into a typical fusiform shape on TGF-β3/CS, and continue growing and reproducing.

In vitro experiments revealed that TGF-β3/CS does not significantly promote or inhibit the growth and proliferation of hPDLSCs, but promotes osteogenic differentiation of hPDLSCs. In vivo experiments verified that hPDLSCs on TGF-β3/CS can survive in animals for a long time. This means TGF-β3/CS has stable biological properties and good biocompatibility, indicating its promise as a biomedical material for future tissue engineering.

Osteogenic differentiation of cells is a complex process involving cell proliferation, extracellular matrix maturation, and mineralization [37]. ALP is an enzyme on the cell membrane that can catalyze the hydrolysis of phosphate esters. Its activity can reflect the osteogenic activity and function of cells, and it has the highest expression during the maturity of the extracellular matrix. Therefore, ALP is

one of the important indicators for evaluating the degree of early osteogenic differentiation of cells. According to the results of ALP staining and its quantitative detection, ALP activity in the TGF-β3 (250 ng/mL)/CS induction group on the seventh day was significantly higher than in the other groups. Compared with day 7, ALP activity increased at day 14, which is not consistent with the results of ALPL expression measured by Western blot. This may be due to ALP being a marker of early osteogenic differentiation of cells, and when cells begin to enter the late stage of osteogenic differentiation, the ALP secreted by the cells may be accumulated in the supernatant, resulting in an increase in ALP content. Alizarin red staining is a common method for identifying advanced osteogenic differentiation of cells [32]. hPDLSCs were cultivated in osteogenic differentiation medium and stained with alizarin red after cultivation for 14 days, showing that TGF-β3 promotes osteogenic differentiation. However, hPDLSCs on TGF-β3/CS cannot be stained with alizarin red to detect calcium ion content, since the high-porosity chitosan material has an adsorption effect on the alizarin red dyeing solution, so the interference of the material itself cannot be ruled out after the dyeing. Therefore, we detected and quantified the osteocalcin of hPDLSC in the materials using calcium colorimetry, which indicated that TGF-β3/CS can increase the expression level of calcium in cells. The TGF-β3 (500ng/mL)/CS group had the highest calcium content, demonstrating that a high concentration of TGF-β3 is more favorable for osteogenic differentiation of hPDLSCs in the late stage of differentiation.

The methods of repairing bone defects can be divided into intramembranous osteogenesis and endochondral ossification. The former induces osteoblasts to secrete a bone-like matrix mineralization, whereas the latter induces cartilage cells to produce cartilage matrix and then gradually mineralize to form bone-like matrix. This experiment was conducted to explore the mechanism through which TGF-β3 induces osteogenic differentiation. The representative proteins of osteogenic (COLI and ALPL) and cartilage (COLII) were selected for Western blot detection. COLI plays an indispensable role in extracellular matrix maturation and formation of mineralized nodules, and is one of the markers of early osteogenic differentiation of cells [38]. COLII is a major component of hyaline cartilage and plays a key role in maintaining chondrocyte function; COLII is one of the important indicators of chondrogenic differentiation. TGF-β3 contributes to the significant improvement in the formation of type II collagen, inducing and promoting cartilage differentiation [39]. According to the Western blot results, the expression of COLI in each group was up-regulated with the prolongation of culture time, and the expression level of COLI in the TGF-β3 (500ng/mL)-induced group was higher than in the control group. The expression of COLII began to increase gradually and the expression of COLII in the seven-day TGF-β3-induced group was significantly higher than in the COLI group. This may be due to TGF-β3 promoting cell differentiation into cartilage in the early stage of cell differentiation. However, the expression levels of COLII were down-regulated in all induction groups, whereas the expression levels of COLI were up-regulated. This may be due to the initiation of endochondral ossification in the TGF-β3-induced group and the entry into the mineralization phase of the cells. Endochondral ossification [40] refers to the process of depositing collagen and non-collagen on the cartilage to mineralize. Here, the cartilage proliferates, matures, and hypertrophies, and then the hypertrophic cartilage matrix is gradually replaced by trabecular bone. A decrease in the expression level of COLII was reported to indicate a stage in which endochondral ossification enters the cartilage matrix calcification [41]. Another study [42] found that TGF-β3 can induce the ossification of human adipose stromal cells into bone tissue in the rat bone defect model, and the trend in COLI and COLII protein expression is basically consistent with the results of this experiment.

Studies have shown that bioactive molecules promote the proliferation, migration, and osteogenic differentiation of PDLSCs by activating the MAPK pathway in vitro [32-34]. Through contrastive analysis of the mechanism of osteogenic differentiation of TGF-β3 and hPDLSCs, we hypothesize that TGF-β3 may act through binding TGF-βRI/II to first start downstream molecule p38 phosphorylation. Following TGF-β3 induction, the p38 MAPK pathways converge at Runx2 to control hPDLSCs differentiation. However, Runx2 is the earliest and continuously expressed protein in the process of cell osteogenesis, marking the beginning of osteogenic differentiation. As shown by the Western blot results, the day 14 expression was significantly lower than on day 7. This trend is consistent with the results reported by Paolella et al. [43]. Other studies [44] have shown that Runx2 plays an important role in coordinating multiple signals involved in osteoblast differentiation and is a specific transcriptional regulator necessary for

osteoblast differentiation and bone formation. The existence of the p38 MAPK pathway was verified by the Western blot results, but the associated protein TAK1 was not detected, potentially because other pathways can bypass this protein, enter the downstream, and finally result in osteogenesis, but this remains to be further verified.

4. Materials and Methods

4.1. Preparation and Characterization of TGF-β3/CS

CS (molecular weight, 3.6 ×10^3 Da; deacetylation degree, 50%) was purchased from Zhengzhou Kerui Fine Chemical Co., Ltd (Zhengzhou, China). TGF-β3 was supplied by the Biopharmaceutical R&D Center of Jinan University (Guangzhou, China). All other chemical reagents obtained from Shanghai Lingfeng were of analytical grade. Briefly, after CS (1% *w*/*v*) was lyophilized, we placed it in a 95% ethanol solution for 2 h and then discarded the ethanol. Next, it was immersed and cleaned in 10% sodium hydroxide solution for 2 h, then repeatedly cleaned with deionized water until the pH was about 7. We produced a lyophilized sponge-like biomaterial that was sterilized and stored for later use. TGF-β3 at different concentrations (0, 62.5, 250, and 500 ng/mL) were loaded on CS by drop.

The water absorption rate, the swelling ratio, and the porosity of CS were calculated as previously reported [45]. The micromorphology of the prepared CS was observed by scanning electron microscopy (SEM, XL30; Philips, Amsterdam, Netherlands).

4.1.1. Release Profile of TGF-β3 from CS

The release of TGF-β3 from CS was measured with ELISA (CUSABIO, Wuhan, China). The scaffold (3 replicates/group) was placed in a 1.5 mL Eppendorf tube, 1 mL MEM was added, which was incubated at 37 °C for 35 days. We collected 1 mL of MEM supernatant and 1 mL fresh MEM was added at day 1, 3, 7, 14, 21, 28, and 35. The supernatant samples were maintained at –80 °C until use for ELISA measurements. ELISA was performed according to the manufacturer's protocol. Light absorbance was read with a microreader at a wavelength of 450 nm (Thermo Lab systems, Waltham, MA, USA).

4.2. Culture of hPDLSCs

The hPDLSCs were obtained from tissues attached to the middle third of the tooth root from healthy 15–20 year old patients (5 men and 5 women) as described previously, who were undergoing orthodontic treatment at the First Affiliated Hospital of Jinan University [46]. All the experimental protocols used were approved by the Ethics Committee of Jinan University (Guangdong, China). The tissues were cut, digested, and cultured with medium supplemented with α-MEM (Gibco, New York, USA), 10% fetal bovine serum (FBS, Gibco, New York, USA), 100 mg/mL streptomycin, and 100U/mL penicillin (MDBio, Shanghai, China) at 37°C in an atmosphere containing 5% CO_2. The medium was changed every 3 days and hPDLSCs at passages (P) 3–5 were used in the following experiments.

4.3. Bioactivity and Biocompatibility Assay

4.3.1. MTT Assay to Test Biocompatibility In Vitro

The cytotoxicity of the CS was evaluated using an extraction test. The ratio between the sample surface and the volume of the medium was 0.5 cm^2/mL. In brief, the 3T3 cells (provided by China National Institute for the Control of Pharmaceutical and Biological Products, Beijing, China) were cultured in a 96-well plate at a density of 1 × 10^4 cells/well in DMEM and 10% FBS for 24 h. The cells were then divided into five groups and separately treated with 25% CS extract, 50% CS extract, 75% CS extract, 100% CS extract, or a blank control of extract alone. At days 1, 2, and 3 of incubation, the proliferative capacity of the cells in each group was examined using the MTT method [45].

4.3.2. Cell Proliferation Assay of hPDLSCs Loaded on TGF-β3/CS

Five different concentrations of TGF-β3 (0, 12, 62.5, 250, and 1000 ng/mL) were loaded on CS. hPDLSCs were seeded in 24-well plates preloading TGF-β3/CS at a density of 2×10^4 cells/well. The viability of the cells was determined using a CCK-8 assay (Enhanced Cell Counting Kit-8, Beyotime, Shanghai, China).

hPDLSCs were seeded in 96-well plates at a density of 5×10^3 cells/well, then treated with different concentrations of TGF-β3 (0, 12, 62.5, 250, 500, and 1000 ng/mL). Cell proliferation was evaluated using an MTT assay.

A microplate reader (Thermo Lab systems, Waltham, MA, USA) was used to detect the absorbance at 570nm (MTT assay) or 450 nm (CCK-8 assay) after shaking samples for 5 min. Each assay was performed in triplicate.

4.3.3. Growth of hPDLSCs Implanted in TGF-β3/CS

To further study cell growth on TGF-β3/CS, hPDLSCs were cultured on TGF-β3/CS for 3 days and stained by Calcein AM/PI (Calcein-AM/PI Double Stain Kit, Shanghai, China), followed by fluorescence microscopy (LSM700, Zeiss, Jena, Germany) to observe the fluorescence degree.

hPDLSCs pre-stained with CM-Dil (BestBio, Shanghai, China) were loaded on TGF-β3/CS and implanted subcutaneously into Sprague–Dawley (SD) rats (280 ± 20 g, male, n = 15; no. 37009200016139) for 7, 14, and 21 days. Animals were sacrificed at 2 and 4 weeks. All the procedures for mice handling were based on the principles (ref 006939801/2010-00810) of Laboratory Animal Care formulated by the National Society for Medical Research and approved by the Ethics Review Committee for Animal Experimentation of Jinan University (ethical review no. 2019346), Guangzhou, China. Experiments complied with the National Institutes of Health guide for the care and use of Laboratory animals (NIH Publications No. 8023, revised 1996). Samples were harvested with the surrounding tissue, followed by examination with fluorescence microscopy (LSM700, Zeiss, Jena, Germany) to observe the fluorescence degree.

4.4. Induction of Osteogenic Differentiation

hPDLSCs (P3) were seeded into 12-well plates at 5×10^4 cells/well and cultured until they reached 80% confluence. Then, hPDLSCs were cultivated in osteogenic differentiation medium, containing 10^{-8} M dexamethasone (Sigma-Aldrich, St. Louis, MO, USA), 10 mM β-glycerophosphate (Sigma-Aldrich, St. Louis, Missouri, USA), and 50 ng/mL ascorbic acid (Sigma-Aldrich, St. Louis, MO, USA) in α-MEM with 10% FBS and 1% penicillin-streptomycin. The osteogenic medium was changed every 2 days.

Induction of hPDLSCs was completed with different concentrations of TGF-β3 (0, 62.5, 250, and 500 ng/mL). After cultivation for 3 and 7 days, we stained the hPDLSCs with an Alkaline phosphatase (ALP) staining kit (Beyotime Institute of Biotechnology, Shanghai, China) to ensure early osteogenic differentiation capacity. After cultivation for 14 days, we stained the hPDLSCs with alizarin red (Cyagen Biosciences, CA, USA) to ensure the late osteogenic differentiation capacity of hPDLCs.

Four different concentrations of TGF-β3 (0, 62.5, 250, and 500 ng/mL) were loaded in CS. After cultivation for 3, 7, and 14 days, we determined the ALP activity of hPDLSCs on TGF-β3/CS using an ALP staining kit (Beyotime Institute of Biotechnology, Shanghai, China). For the detection and quantification of osteocalcin in hPDLSCs in the late stage of each group of materials, a calcium colorimetric assay (Sigma-Aldrich, St. Louis, MO, USA) was used after cultivation for 14, 21, and 28 days.

4.5. Western Blot Analysis

After 7 and 14 days of cultivation, cells were digested and collected. The cell pellets were lysed in a RIPA buffer (Cell Signaling Technology, Beverly, MA, USA) on ice for 30 mins, and then centrifuged at 12,000 rpm and 4 °C for 30 min. The supernatants were collected, and the protein concentrations were measured with a BCA protein assay kit (Life Technologies, Carlsbad, CA, USA)

according to the manufacturer's instructions. Sodium dodecyl sulfate polyacrylamide gel electrophoresis and immunoblot analysis were conducted according to standard protocols and visualized using the ChemiDoc-It Imaging System (UVP, Upland, MA, USA). The TGF-βRI, TGF-βRII, p38, Pp38, COLI (Affinity Biosciences, OH, USA), ALPL (Alkaline phosphatase), COLII (Abcam, Cambridge, MA, USA), GAPDH antibodies, and their phosphorylated patterns, as well as HRP-conjugated secondary antibody (Cell Signaling Technology, Boston, MA, USA) were used.

4.6. Statistical Analysis

Data are reported as mean ± standard deviation. To evaluate the statistical significance of the data, groups were compared in GraphPad Prism 6 (GraphPad Software Inc., La Jolla, CA, USA) by one-way analysis of variance (ANOVA) followed by Tukey's test. P values < 0.05 were considered statistically significant.

5. Conclusions

TGF-β3 had no effect on the proliferation of hPDLSCs, but an appropriate concentration of TGF-β3 could promote the osteogenic differentiation of hPDLSCs via activation of the p38 MAPK pathway. The prepared TGF-β3/CS has a good water absorption rate, swelling ratio, and porosity; is favorable for the adhesion, spreading and growth of seed cells; has good biosafety; and conforms to the medical standard of biological materials. TGF-β3/CS can promote the osteogenic differentiation of hPDLSCs, and the combination of the two is expected to be used for the repair of alveolar bone defects.

Acknowledgments: This work was supported by the Major Scientific and Technological Special Project of the Administration of Ocean and Fisheries of Guangdong Province (GDME-2018C013, Yuecainong, 2017, no.17), Guangzhou Science and Technology Program key projects (201803010044) and Science and technology program of Tianhe District, Guangzhou City (201704YG066).

Conflicts of Interest: The authors declare no conflicts of interest.

References

1. Goker, F.; Larsson, L.; Del Fabbro, M.; Asa'ad, F. Gene delivery therapeutics in the treatment of periodontitis and peri-implantitis: A state of the art review. *Int J Mol Sci* **2019**, *20*.
2. Shanbhag, S.; Pandis, N.; Mustafa, K.; Nyengaard, J.R.; Stavropoulos, A. Alveolar bone tissue engineering in critical-size defects of experimental animal models: A systematic review and meta-analysis. *Journal of tissue engineering and regenerative medicine* **2017**, *11*, 2935-2949.
3. Larsson, L.; Decker, A.M.; Nibali, L.; Pilipchuk, S.P.; Berglundh, T.; Giannobile, W.V. Regenerative medicine for periodontal and peri-implant diseases. *Journal of dental research* **2016**, *95*, 255-266.
4. Al-Askar, M.; Alsaffar, D. Feasibility of using allograft bone with resorbable collagen membrane for alveolar ridge vertical defect augmentation for dental implant placement in patient with aggressive periodontitis: A case report. *Saudi Dent J* **2018**, *30*, 256-259.
5. Akintoye, S.O. The distinctive jaw and alveolar bone regeneration. *Oral Dis* **2018**, *24*, 49-51.
6. EzEldeen, M.; Wyatt, J.; Al-Rimawi, A.; Coucke, W.; Shaheen, E.; Lambrichts, I.; Willems, G.; Politis, C.; Jacobs, R. Use of cbct guidance for tooth autotransplantation in children. *Journal of dental research* **2019**, *98*, 406-413.
7. Gjerde, C.; Mustafa, K.; Hellem, S.; Rojewski, M.; Gjengedal, H.; Yassin, M.A.; Feng, X.; Skaale, S.; Berge, T.; Rosen, A., *et al.* Cell therapy induced regeneration of severely atrophied mandibular bone in a clinical trial. *Stem cell research & therapy* **2018**, *9*, 213.
8. Kloss, F.R.; Offermanns, V.; Kloss-Brandstatter, A. Cecomparison of allogeneic and autogenous bone grafts for augmentation of alveolar ridge defects-a 12-month retrospective radiographic evaluation. *Clin Oral Implants Res* **2018**.
9. Hameed, M.H.; Gul, M.; Ghafoor, R.; Khan, F.R. Vertical ridge gain with various bone augmentation techniques: A systematic review and meta-analysis. *J Prosthodont* **2019**.
10. Iviglia, G.; Kargozar, S.; Baino, F. Biomaterials, current strategies, and novel nano-technological approaches for periodontal regeneration. *Journal of functional biomaterials* **2019**, *10*.
11. Urban, I.A.s.; Montero, E.; Monje, A.; Sanz-Sanchez, I. Effectiveness of vertical ridge augmentation interventions. A systematic review and meta-analysis. *J Clin Periodontol* **2019**.

12. Reynolds, M.A.; Kao, R.T.; Camargo, P.M.; Caton, J.G.; Clem, D.S.; Fiorellini, J.P.; Geisinger, M.L.; Mills, M.P.; Nares, S.; Nevins, M.L. Periodontal regeneration - intrabony defects: A consensus report from the aap regeneration workshop. *Journal of periodontology* **2015**, *86*, S105-107.
13. Bottino, M.C.; Thomas, V.; Schmidt, G.; Vohra, Y.K.; Chu, T.M.; Kowolik, M.J.; Janowski, G.M. Recent advances in the development of gtr/gbr membranes for periodontal regeneration--a materials perspective. *Dental materials : official publication of the Academy of Dental Materials* **2012**, *28*, 703-721.
14. Rakhmatia, Y.D.; Ayukawa, Y.; Furuhashi, A.; Koyano, K. Current barrier membranes: Titanium mesh and other membranes for guided bone regeneration in dental applications. *J Prosthodont Res* **2013**, *57*, 3-14.
15. Soldatos, N.K.; Stylianou, P.; Koidou, V.P.; Angelov, N.; Yukna, R.; Romanos, G.E. Limitations and options using resorbable versus nonresorbable membranes for successful guided bone regeneration. *Quintessence Int* **2017**, *48*, 131-147.
16. Sasaki, H.; Rothrauff, B.B.; Alexander, P.G.; Lin, H.; Gottardi, R.; Fu, F.H.; Tuan, R.S. In vitro repair of meniscal radial tear with hydrogels seeded with adipose stem cells and tgf-beta3. *The American journal of sports medicine* **2018**, *46*, 2402-2413.
17. Lee, H.L.; Yu, B.; Deng, P.; Wang, C.Y.; Hong, C. Transforming growth factor-beta-induced kdm4b promotes chondrogenic differentiation of human mesenchymal stem cells. *Stem Cells* **2016**, *34*, 711-719.
18. Yang, Q.; Teng, B.H.; Wang, L.N.; Li, K.; Xu, C.; Ma, X.L.; Zhang, Y.; Kong, D.L.; Wang, L.Y.; Zhao, Y.H. Silk fibroin/cartilage extracellular matrix scaffolds with sequential delivery of tgf-beta3 for chondrogenic differentiation of adipose-derived stem cells. *International journal of nanomedicine* **2017**, *12*, 6721-6733.
19. Jing, H.; Zhang, X.; Gao, M.; Luo, K.; Fu, W.; Yin, M.; Wang, W.; Zhu, Z.; Zheng, J.; He, X. Kartogenin preconditioning commits mesenchymal stem cells to a precartilaginous stage with enhanced chondrogenic potential by modulating jnk and beta-catenin-related pathways. *FASEB journal : official publication of the Federation of American Societies for Experimental Biology* **2019**, fj201802137RRR.
20. Grafe, I.; Alexander, S.; Peterson, J.R.; Snider, T.N.; Levi, B.; Lee, B.; Mishina, Y. Tgf-beta family signaling in mesenchymal differentiation. *Cold Spring Harbor perspectives in biology* **2018**, *10*.
21. Deng, M.; Mei, T.; Hou, T.; Luo, K.; Luo, F.; Yang, A.; Yu, B.; Pang, H.; Dong, S.; Xu, J. Tgfbeta3 recruits endogenous mesenchymal stem cells to initiate bone regeneration. *Stem cell research & therapy* **2017**, *8*, 258.
22. Ripamonti, U.; Dix-Peek, T.; Parak, R.; Milner, B.; Duarte, R. Profiling bone morphogenetic proteins and transforming growth factor-betas by htgf-beta3 pre-treated coral-derived macroporous bioreactors: The power of one. *Biomaterials* **2015**, *49*, 90-102.
23. Ripamonti, U. Developmental pathways of periodontal tissue regeneration: Developmental diversities of tooth morphogenesis do also map capacity of periodontal tissue regeneration? *Journal of periodontal research* **2019**, *54*, 10-26.
24. Klar, R.M.; Duarte, R.; Dix-Peek, T.; Ripamonti, U. The induction of bone formation by the recombinant human transforming growth factor-beta3. *Biomaterials* **2014**, *35*, 2773-2788.
25. Ripamonti, U.; Ramoshebi, L.N.; Teare, J.; Renton, L.; Ferretti, C. The induction of endochondral bone formation by transforming growth factor-?3: Experimental studies in the non-human primate papio ursinus. *Journal of cellular and molecular medicine* **2007**, *ja*.
26. Ripamonti, U.; Duarte, R.; Ferretti, C. Re-evaluating the induction of bone formation in primates. *Biomaterials* **2014**, *35*, 9407-9422.
27. Moioli, E.K.; Clark, P.A.; Sumner, D.R.; Mao, J.J. Autologous stem cell regeneration in craniosynostosis. *Bone* **2008**, *42*, 332-340.
28. Gupta, A.; Rattan, V.; Rai, S. Efficacy of chitosan in promoting wound healing in extraction socket: A prospective study. *J Oral Biol Craniofac Res* **2019**, *9*, 91-95.
29. Safari, S.; Mahdian, A.; Motamedian, S.R. Applications of stem cells in orthodontics and dentofacial orthopedics: Current trends and future perspectives. *World J Stem Cells* **2018**, *10*, 66-77.
30. Abdel Meguid, E.; Ke, Y.; Ji, J.; El-Hashash, A.H.K. Stem cells applications in bone and tooth repair and regeneration: New insights, tools, and hopes. *Journal of cellular physiology* **2018**, *233*, 1825-1835.
31. Kim, S.H.; Kim, K.H.; Seo, B.M.; Koo, K.T.; Kim, T.I.; Seol, Y.J.; Ku, Y.; Rhyu, I.C.; Chung, C.P.; Lee, Y.M. Alveolar bone regeneration by transplantation of periodontal ligament stem cells and bone marrow stem cells in a canine peri-implant defect model: A pilot study. *Journal of periodontology* **2009**, *80*, 1815-1823.
32. Ge, B.; Liu, H.; Liang, Q.; Shang, L.; Wang, T.; Ge, S. Oxytocin facilitates the proliferation, migration and osteogenic differentiation of human periodontal stem cells in vitro. *Arch Oral Biol* **2019**, *99*, 126-133.

33. Zhu, Y.; Li, Q.; Zhou, Y.; Li, W. Tlr activation inhibits the osteogenic potential of human periodontal ligament stem cells through akt signaling in a myd88- or trif-dependent manner. *Journal of periodontology* **2018**.
34. Wang, L.; Wu, F.; Song, Y.; Duan, Y.; Jin, Z. Erythropoietin induces the osteogenesis of periodontal mesenchymal stem cells from healthy and periodontitis sources via activation of the p38 mapk pathway. *International journal of molecular medicine* **2018**, *41*, 829-835.
35. Chen, G.; Deng, C.; Li, Y.P. Tgf-beta and bmp signaling in osteoblast differentiation and bone formation. *Int J Biol Sci* **2012**, *8*, 272-288.
36. Feldman, D.S.; McCauley, J.F. Mesenchymal stem cells and transforming growth factor-beta(3) (tgf-beta(3)) to enhance the regenerative ability of an albumin scaffold in full thickness wound healing. *Journal of functional biomaterials* **2018**, *9*.
37. Menon, A.H.; Soundarya, S.P.; Sanjay, V.; Chandran, S.V.; Balagangadharan, K.; Selvamurugan, N. Sustained release of chrysin from chitosan-based scaffolds promotes mesenchymal stem cell proliferation and osteoblast differentiation. *Carbohydrate polymers* **2018**, *195*, 356-367.
38. Yu, W.; Jiang, D.; Yu, S.; Fu, J.; Li, Z.; Wu, Y.; Wang, Y. Sall4 promotes osteoblast differentiation by deactivating notch2 signaling. *Biomedicine & pharmacotherapy = Biomedecine & pharmacotherapie* **2018**, *98*, 9-17.
39. Lin, C.Y.; Chang, Y.H.; Li, K.C.; Lu, C.H.; Sung, L.Y.; Yeh, C.L.; Lin, K.J.; Huang, S.F.; Yen, T.C.; Hu, Y.C. The use of ascs engineered to express bmp2 or tgf-beta3 within scaffold constructs to promote calvarial bone repair. *Biomaterials* **2013**, *34*, 9401-9412.
40. McDermott, A.M.; Herberg, S.; Mason, D.E.; Collins, J.M.; Pearson, H.B.; Dawahare, J.H.; Tang, R.; Patwa, A.N.; Grinstaff, M.W.; Kelly, D.J., *et al*. Recapitulating bone development through engineered mesenchymal condensations and mechanical cues for tissue regeneration. *Science translational medicine* **2019**, *11*.
41. Aisenbrey, E.A.; Bryant, S.J. The role of chondroitin sulfate in regulating hypertrophy during msc chondrogenesis in a cartilage mimetic hydrogel under dynamic loading. *Biomaterials* **2019**, *190-191*, 51-62.
42. Guerrero, J.; Pigeot, S.; Muller, J.; Schaefer, D.J.; Martin, I.; Scherberich, A. Fractionated human adipose tissue as a native biomaterial for the generation of a bone organ by endochondral ossification. *Acta biomaterialia* **2018**, *77*, 142-154.
43. Paolella, F.; Gabusi, E.; Manferdini, C.; Schiavinato, A.; Lisignoli, G. Specific concentration of hyaluronan amide derivative induces osteogenic mineralization of human mesenchymal stromal cells: Evidence of runx2 and col1a1 genes modulation. *Journal of biomedical materials research. Part A* **2019**.
44. Douglas, T.E.L.; Vandrovcova, M.; Krocilova, N.; Keppler, J.K.; Zarubova, J.; Skirtach, A.G.; Bacakova, L. Application of whey protein isolate in bone regeneration: Effects on growth and osteogenic differentiation of bone-forming cells. *J Dairy Sci* **2018**, *101*, 28-36.
45. Zang, S.; Dong, G.; Peng, B.; Xu, J.; Ma, Z.; Wang, X.; Liu, L.; Wang, Q. A comparison of physicochemical properties of sterilized chitosan hydrogel and its applicability in a canine model of periodontal regeneration. *Carbohydrate polymers* **2014**, *113*, 240-248.
46. Yoshio, S.; Hiroaki, T.; Masahide, T.; Kenichiro, M.; Tomomi, N.; Keigo, S.; Mariko, K.; Toshihito, A.; Hiroyuki, O.; Takanobu, K. Fibroblast growth factor-2 stimulates directed migration of periodontal ligament cells via pi3k/akt signaling and cd44/hyaluronan interaction. *Journal of Cellular Physiology* **2011**, *226*, 809-821.